Article

Fast Synthesis of Graphene Oxide–β-Lactam as a Residue-Free Environmental Bacterial Inhibitor

Chenyan Hu,[⊥] Pengfei Heng,[⊥] Yuanyuan Zeng, Qing Zhang, Meilian Zhao, Zhongzhu Yang,* and Yang He*

Read Online

ACCESS | Metrics & More | Article Recommendations | Supporting Information

ABSTRACT: Common pathogenic bacteria contaminate the environment through various modes of transmission. It is thus crucial to develop simple preparation methods of residue-free environmental disinfectants. β-Lactam antibiotics are frequently prescribed in clinical practice to treat bacterial infections. In this study, we used electrochemical exfoliation to synthesize graphene oxide (GO) with abundant ketene functional groups. A residue-free GO−β-lactam (GOβL) was subsequently obtained by mixing ketene and azomethine-H via a [2 + 2] cycloaddition reaction in the aqueous phase. GOβL has shown broad-spectrum bacterial inhibition against four bacteria (*Staphylococcus aureus*, *Escherichia coli*, *Salmonella enterica*, and *Shigella dysenteriae*), and it degrades rapidly within 24 h. This study provides a fast and easy method for the synthesis of GOβL, which can be employed as a promising environmental bacteriostatic disinfectant in real-life applications.

Binding of GOβL to bacteria

Results of molecular simulations of inhibition sites
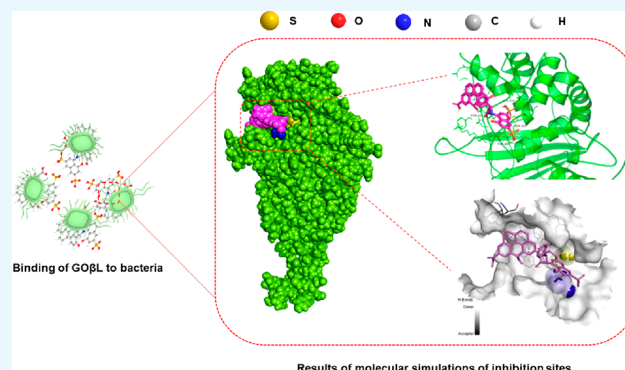
1. INTRODUCTION

Common pathogenic bacteria, such as *Staphylococcus aureus*, *Escherichia coli*, *Salmonella enterica*, and *Shigella dysenteriae*, can cause epidemics of various diseases. These bacteria spread through soil, air, water, and human-to-human contact, increasing the susceptibility of environmental water and food ingredients to bacterial contaminations.[1,2] It is thus extremely important to enhance our quality of life with environmental bacterial inhibitors because of the ubiquity of pathogenic bacteria.[3,4]

Common environmental disinfectants, including chlorine-containing, peroxide-based, alcohol-based, and iodine-containing disinfectants, can be applied to disinfect the air, water, food processing plants, and other susceptible environments.[5] However, numerous environmental disinfectants tend to cause pollution because of their nondegradable nature and long-term presence in the environment.[6] It is thus crucial to develop simple preparation methods of residue-free environmental disinfectants. β-Lactam antibiotics are important heterocycles with broad antimicrobial activity and are currently the most widely applied class of antimicrobial drugs used against infectious diseases. The β-lactam ring is a common structural feature of numerous antibiotics, such as penicillins, cephalosporins, and carbapenems, extensively adopted for treating bacterial infections.[7] However, the massive use of β-lactam antibiotics in recent years and the structural consistency of the antibiotics have led to the development of specific β-lactamases, causing bacterial resistance.[8,9] Novel and accessible preparation methods of β-lactam-based antibacterial agents are thus urgently required.[10]

Graphene oxide (GO) is a widely studied new material in life sciences with excellent water solubility and high specific surface area.[11,12] Its monolayer two-dimensional honeycomb structure enables its use as an excellent substrate for preparing photocatalytic materials, multifunctional electrochemical composites, and bacterial inhibitors.[13,14] Sengupta et al. demonstrated that GO could enhance the bacteriostatic effect of composites through the self-assembly of La ions on their surfaces because the synthesized inhibitors interact with bacterial cell membranes to produce a bactericidal effect.[15] In addition, Jiang et al. constructed a novel graphene coating with photothermal properties for bactericidal applications.[16] Despite the excellent antibacterial properties of these graphene-based complexes, their practical application is hindered by their sophisticated synthesis steps and light-dependent bactericidal behavior.

In this study, GOβL was prepared by the $[2 + 2]$ cycloaddition reaction of GO and azomethine-H in the aqueous phase. The abundant ketene functional groups on the surface of GO offer a large specific surface area and modification sites, allowing GO to serve as a favorable substrate for the preparation of bacterial inhibitors. To the best of our knowledge, this is the first report of a monocyclic GOβL. This study provides a fast and facile approach for the synthesis of β-lactam antibiotics, and the prepared GOβL appears to be promising as an effective environmental bacteriostatic disinfectant.

2. MATERIALS AND METHODS

2.1. Bacterial Strains and Culture Conditions. Four standard bacterial strains, *S. aureus* [American Type Culture Collection (ATCC) 25923], *E. coli* (ATCC 25922), *S. enterica* (ATCC 14028), and *S. dysenteriae* [National Center for Medical Culture Collections (CMCC) (B) 51105], were used in this study. Their environmental counterparts isolated from local wet markets in Chengdu were also included in the study. These environmental isolates were collected following the entry–exit inspection and quarantine industry standards of the People's Republic of China and identified by Prof. Qing Zhang of Xihua University. All bacterial strains were grown in Mueller-Hinton broth (MHB) medium for 12 h at 37 °C (shaking at 200 rpm). The bacterial biomass of each culture was then washed twice with phosphate-buffered saline (PBS) to remove the medium after incubation.

2.2. Synthesis of GOβL. Two pencil cores (0.58 g) were used as the anode and cathode in an electrolysis cell filled with saturated NaCl solution (200 mL). A constant potential of 3 V with a current of 0.06 mA was applied to the two electrodes and was maintained for 24 h, yielding the sample "GO". Nitrogen gas was subsequently passed through the GO solution to remove the chlorine gas generated during electrolysis, a process that takes place in 1 h. GOβL was finally prepared by mixing 0.02 M azomethine-H solution (20 mL, solvent: distilled water) with the aerated GO (60 mL, solvent: distilled water) for 20 min (25 °C) via a $[2 + 2]$ cycloaddition reaction.

2.3. Characterization of GO and GOβL. Atomic force microscopy (AFM) of the GOβL was conducted on a Multimode Nanoscope V scanning probe microscopy system (Bruker, USA). A commercial AFM cantilever tip with a force constant of $\sim$50 N m^{-1} and a resonance vibration frequency of $\sim$350 kHz was used in the test. The ultraviolet–visible (UV–vis) absorption spectra and Fourier transform infrared spectroscopy (FT-IR) spectra of GO and GOβL were obtained using a MAPADA UV6300 UV–vis spectrophotometer (Shanghai, China) and a NICOLET 5700 FT-IR spectrometer (Waltham, USA), respectively. For the FT-IR measurements, samples were prepared by grinding GO/GOβL dry powder with KBr and then compressed into a thin slice. Raman scattering of the GO/GOβL was performed using an Almega Thermal Nicolet dispersive Raman spectrometer with the second harmonic (785 nm) of the Nd:YLF laser source. The X-ray photoelectron spectroscopy (XPS) pattern of the samples was subsequently measured on a Thermo ESCALAB 250XI scanning XPS microscope using a monochromatic Al Kα X-ray (1486.6 eV) source. The backgrounds of the atomic spectra were removed by Shirley background subtraction before deconvolution.

2.4. Evaluation of the Antibacterial Activities of GOβL in Standard Bacterial Strains and Environmental Isolates. The minimum inhibitory concentration (MIC) represents the lowest concentration of an antibacterial drug that can inhibit the visible growth of bacteria. Cultures of the four standard bacterial strains and four environmental isolates were first adjusted to approximately 1.5×10^8 CFU mL^{-1}, and the GOβL stock solution was diluted following a concentration gradient to seven concentrations of 148.5, 92.4, 63.5, 48.9, 42.0, 38.1, and 36.1 μg mL^{-1}. Each bacteria (100 μL) and seven different concentrations of GOβL (100 μL) were added sequentially to a 96-well plates and mixed and incubated for 18 h at 37 °C in an incubator. The absorbance of the cultures was determined using a HEALES MB-580 enzyme analyzer (Shenzhen, China), and the MIC assay results were finally analyzed based on optical density (OD) at 630 nm. These experiments were performed in triplicate and repeated three times.

2.5. Evaluation of the Degradation Effect of GOβL. The UV–vis absorption spectra of GOβL stock solution stored at room temperature for 0, 2, 4, 6, 12, and 24 h were measured using a MAPADA UV6300 UV–vis spectrophotometer (Shanghai, China) to determine its degradation effect.

2.6. GOβL Inhibition Site Analysis. The molecular structure of GO was drawn using the ChemDraw Professional software (version 14.0; PerkinElmer Company, Massachusetts, USA). Since the action sites of β-lactam antibiotics have been confirmed to be specific penicillin-binding proteins (PBPs) on bacterial cell membranes,[17] the crystal structure of PBP3 from the RCSB Protein Data Bank (https://www.rcsb.org/) was selected for subsequent GOβL inhibition site simulations. Simulations of GOβL inhibition sites were finally performed using the AutoDock Vina software (version 1.2.0; CCSB Company, California, USA).

3. RESULTS

3.1. Preparation and Characterization of GO and GOβL. GOβL was prepared using a rapid method. The first step was electrochemical exfoliating graphite into GO sheets using low voltage and low current with Cl$_2$ as the oxidant.[18] The ketene groups on GO with ketenyl stretching appeared at 2100–2200 cm^{-1} in the infrared spectra. GOβL was obtained by reacting ketene and azomethine-H in the second step via a $[2 + 2]$ cycloaddition reaction.[19] Figure 1 exhibits AFM images of GO and GOβL. The apparent height of the GO sheet was about 0.628 nm. Notably, there were many anomalous holes of 100–200 nm diameter on the GO sheets, probably caused by repeated oxidation for long hours.[20] Nevertheless, some GO sheets had a small degree of oxidation and were free of holes. The apparent height of GOβL increased to 0.857 nm, suggesting the formation of monocyclic β-lactam structures.[21]

Figure 2a,b shows the FT-IR spectra and UV–vis spectra of GO and GOβL, respectively. Based on the first-principles density functional theory (DFT) calculations (Figure 2c,d), the peaks near 2172 cm^{-1} in the FT-IR spectrum of GO were consistent with the stretching vibration of C=C=O at 2211 cm^{-1} predicted by DFT, indicating the presence of ketene groups at the edges of the GO lamellae. However, only the absorption peak of the $\pi-\pi^*$ transition red-shifted to 295 nm was visible in the UV spectrum of GO,[22,23] probably forming a larger conjugated structure induced by the oxygen-containing functional group.[24] The characterized peak at 1774 cm^{-1} in the FT-IR spectrum of GOβL was ascribed to the formation of the
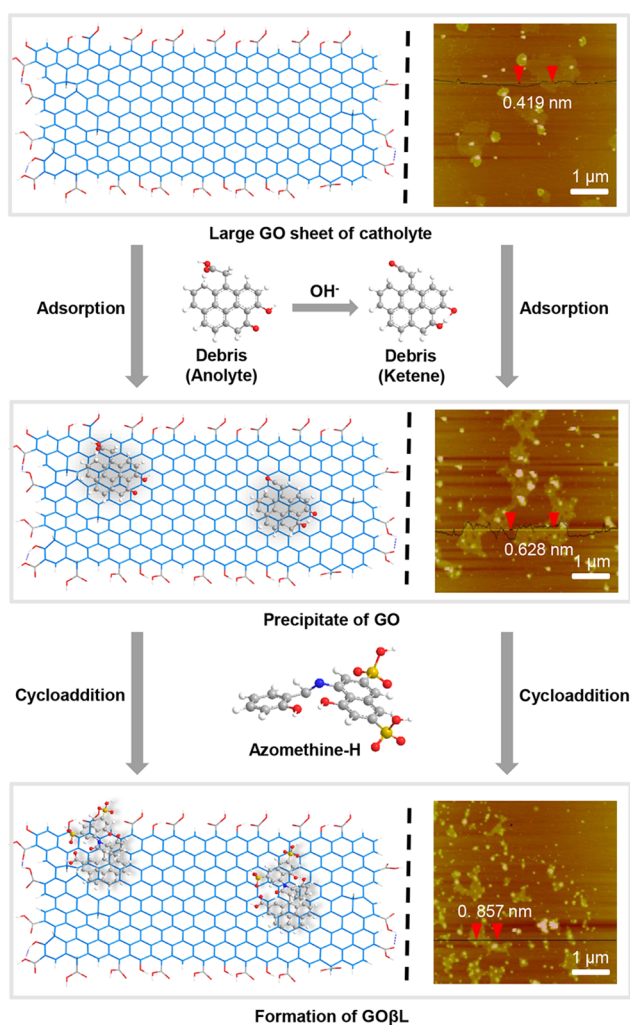
Figure 1. Schematic representation of GOβL formation via a [2 + 2] cycloaddition of GO with azomethane-H. The reaction of ketene functional groups in GO with azomethane-H to form β-lactam ring structures.

monocyclic β-lactam structure, which was also consistent with the IR spectral results (1752 cm^{-1}) obtained through B3LYP/6-31G (d) calculations (Figure 2d). In addition, the reaction of ketene with hydroxyl groups to form esters has also been considered. Calculations from B3LYP/6-31G(d) give a corresponding maximum absorption peak of approximately 1678 cm^{-1} (Figure S5), which differs from the peak formed by the monocyclic β-lactam structure (1774 cm^{-1}). All of the calculations on structure optimizations and vibrational frequencies were carried out with first-principles density functional theory in the Gaussian 09 program package.[25] The UV−vis spectrum of GOβL revealed that the absorption peak at 234 nm corresponded to a π−π* leap in the C=C bond of the aromatic ring, while the small peak near 373 nm corresponded to the quaternary ring structure of the β-lactam. The highest proportional oxygen-containing functional groups based on the XPS spectrum of GO was carboxyl and hydroxyl groups,[11] which provided excellent hydrophilicity to GO (Figure S1). The Raman spectrum of GO (λ$_{ex}$ = 785 nm) had a G-band at 1579 cm^{-1} and a D-band at 1434 cm^{-1} (Figure S2). Of note, the 2D band diverged into two peaks: 2613 and 2714 cm^{-1}, possibly because of two completely different GO structures resulting from electrolysis of carbon rods at the

cathode and anode, including large sheets of GO and small sheets of GO bound to antibiotics (results in agreement with AFM). These findings further proved that ketene was most likely a product of the GO anode electrolyte under alkaline conditions (Figure S3).

3.2. Antibacterial Effect of GOβL in Standard Bacterial Strains and Environmental Isolates. The bacterial inhibitory activity of GOβL was determined based on the MIC. GOβL (63.5 μg mL^{-1}) exhibited a promising broad-spectrum bacterial inhibition against all four common pathogenic bacteria (Gram-positive *S. aureus* and Gram-negative *E. coli*, *S. enterica*, and *S. dysenteriae*), with the best inhibitory effect observed against *S. dysenteriae* (Figure 3). In particular, the MIC of GOβL against *S. dysenteriae* was 48.9 μg mL^{-1}. Both synthetic raw materials, azomethine-H and GO, exhibited poor bacterial inhibition than GOβL (non-antibacterial vs 92.4 μg mL^{-1} vs 63.5 μg mL^{-1}), demonstrating that the bacterial inhibitory effect of GOβL mainly originated from the produced β-lactams.

The relationship between incubation time and the bacterial inhibitory effect of GOβL (63.5 μg mL^{-1}) was determined using the four bacterial strains isolated from the local wet markets in Chengdu to further verify the application potential of GOβL as an environmental bacterial inhibitor (Figure 4). Notably, the calibrated absorbance ($A_{\text{postculture}} - A_{\text{negative control}}$) of the four environmental isolates varied insignificantly due to not reaching the logarithmic growth period in the first 6 h of incubation. However, the inhibitory effect of GO and azomethine-H diminished with an extension of the incubation time to 12 h. *S. aureus* and *E. coli* treated with GO exhibited some bacterial growth. In contrast, azomethine-H had no inhibition against any of the four environmental isolates. Moreover, the inhibitory effect of GOβL on *S. aureus* diminished after prolonging the incubation time to 24 h but remained unchanged on the other three Gram-negative bacteria (*E. coli*, *S. enterica*, and *S. dysenteriae*). Of note, neither GO nor azomethine-H inhibited the growth of the four environmental isolates. However, GOβL still inhibited the three Gram-negative bacteria after 48 h incubation, with an inhibition effect of more than 96%. These findings strongly suggested that the prepared GOβL had an excellent bactericidal effect and strong broad-spectrum antibacterial activity against common environmental pathogens.

3.3. Degradation Effect of GOβL. Though GOβL possesses superior bacterial inhibitory properties enabling its potential utilization as a bacteriostatic agent, its environmental contamination after spraying should be investigated to assess its residual effects. The degradation effect of the synthesized GOβL (42 μg mL^{-1}) with time was thus measured to establish this effect (Figure 5). The freshly synthesized GOβL existed as a distinct UV absorption peak at 373 nm with no overlap with the characteristic peak of azomethine-H (356 nm). However, the characteristic peaks of GOβL were observed to decrease significantly with the extension of time, exhibiting a blue shift phenomenon. Notably, the characteristic peak of GOβL was not observed at its half-life, which was estimated to be about 12 h. However, the characteristic peak of azomethine-H at approximately 356 nm appeared even at 12 h. The content and remaining structure of GOβL stabilized after 24 h of degradation, while the UV spectrum did not vary substantially. The easy degradability of GOβL was attributed to the generated β-lactams being prone to the hydrolysis reaction of ring opening. The presence of natural precipitation and other
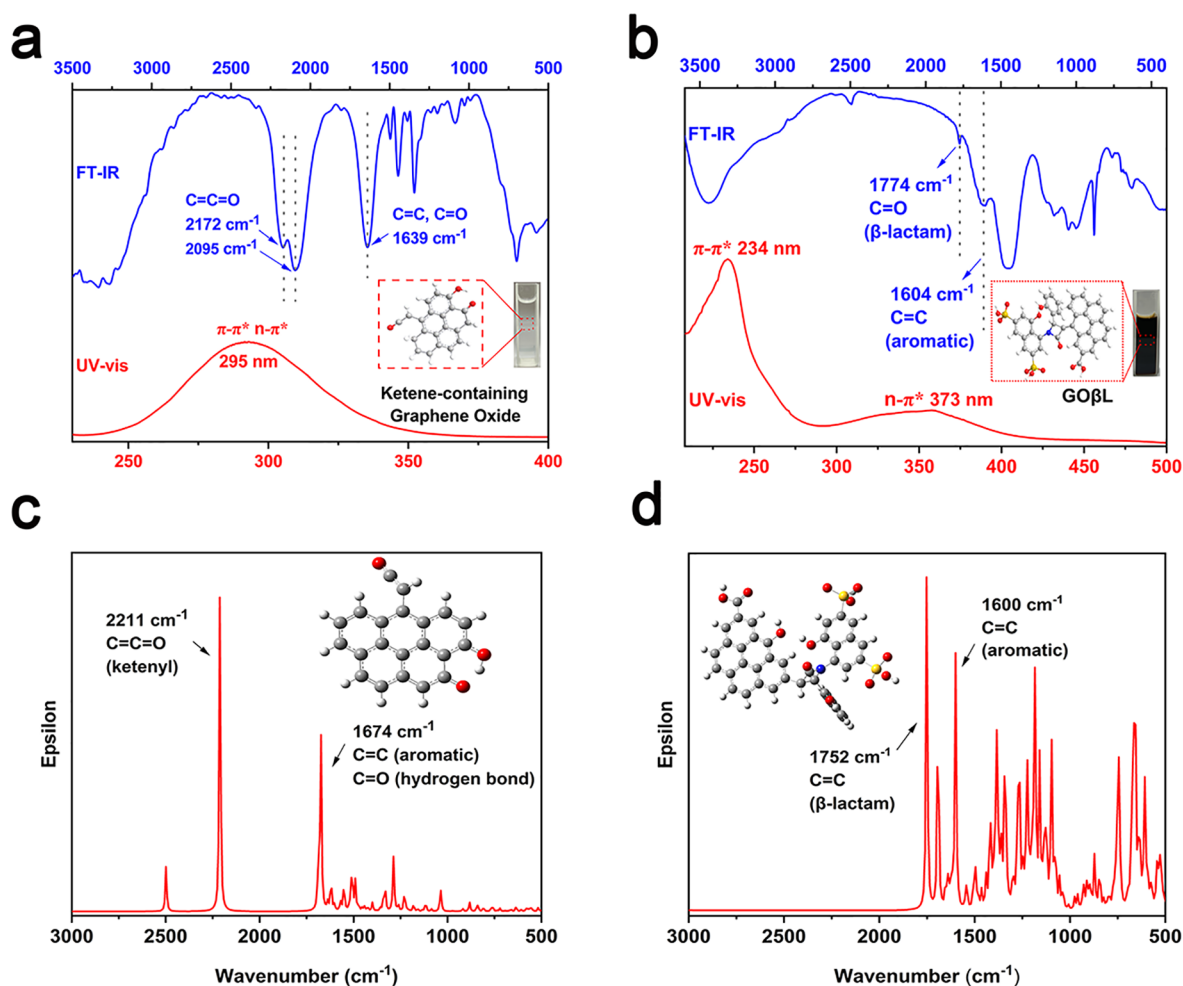
Figure 2. Characterization of GOβL and GO. (a) FT-IR spectra and UV−vis absorption spectra of GO. (b) FT-IR spectra and UV−vis absorption spectra of GOβL. (c) Structure and IR spectra of GO obtained through B3LYP/6-31G(d). (d) IR spectral results obtained through B3LYP/6-31G(d) calculations.

factors in the environment further accelerated the degradation efficiency of GOβL, thus lessening its pollution effect. The antibacterial effect and degradability of GOβL conformed to the expected requirements, permitting its use as an environmental bacterial inhibitor.

3.4. Analysis of GOβL Inhibition Sites. The inhibition sites of GOβL were analyzed using AUTODOCK VINA molecular simulations (Figure 6). The β-lactam ring is covalently bound to the active serine (Ser307) present in PBP3.[21,26,27] It thus interrupts the peptidoglycan monomer cross-linking process and prevents bacteria from synthesizing intact cell walls. Molecular simulations reveal that GOβL can block the channel in front of the active serine binding site and inhibit the entry of peptidoglycan monomers into the active serine site.[28,29] It acts as a peptide chain blocker, leading to the inability to produce an intact cell wall because of the large GO layer in GOβL. In this study, the Gram-positive bacteria (*S. aureus*) were found to be less susceptible to growth inhibition than the Gram-negative bacteria (*E. coli*, *S. enterica*, and *S. dysenteriae*). This phenomenon was attributed to the thick cell wall of Gram-positive bacteria where GOβL could not easily block the channel in front of the active serine binding site and interrupt the cross-linking process.[30] Nevertheless, GOβL still exerts a decent inhibitory effect on Gram-negative bacteria,[26,29] laying a foundation for its application in the environment.

4. DISCUSSION

Environmental pathogenic bacteria contaminate water and food, resulting in human disease. Despite this challenge, the improper and inappropriate use of disinfectants, including their excessive use, poses a potential threat to organisms and ecosystems owing to their numerous side effects.[31,32] It is thus crucial to develop simple preparation methods of residue-free environmental disinfectants.[33,34] β-Lactam antibiotics are commonly used in clinical practice to treat bacterial infections. However, their misuse has caused a gradual rise in bacterial resistance.[35] Previous studies postulate that GO can inhibit bacterial growth by loading metal ions.[22] In this study, GO rich in ketene functional groups and azomethine-H was employed to prepare GOβL via a [2 + 2] cycloaddition reaction in the aqueous phase. Of note, the synthesized GOβL exhibited bacterial inhibition against common pathogenic bacteria in the environment.

The electrochemically exfoliated GO was enriched with ketene functional groups through XPS, FT-IR, UV−vis spectroscopy, and Raman spectroscopy (Figure 2). The synthesized GOβL was also clearly observed as a β-lactam structure through FT-IR (Figure 2). The ketene functional groups of GO express numerous monocyclic lactam ring structures, increasing the concentration of the inhibitory component. GOβL exhibited excellent inhibition against four
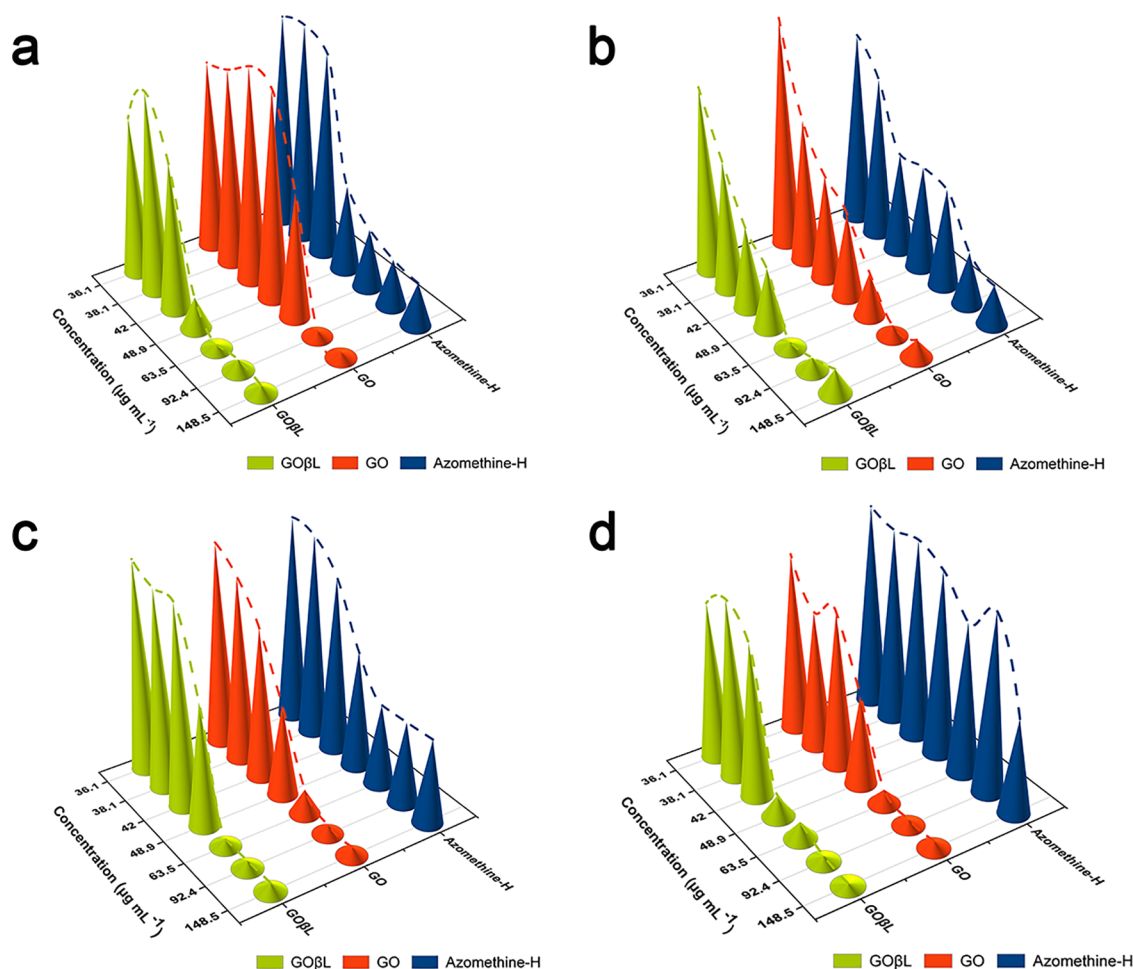
Figure 3. Inhibition of four standard strains after incubation at various concentrations of GOβL. Bacterial inhibition of *S. aureus* (a), *E. coli* (b), *S. enterica* (c), and *S. dysenteriae* (d) by different concentrations of GOβL.

standard bacterial strains and environmental isolates, especially against *S. dysenteriae* (MIC, 48.9 μg mL^{-1}) (Figures 3 and 4). Nevertheless, the inhibitory effect of GOβL on the Gram-positive bacteria (*S. aureus*) was weaker than that on the Gram-negative bacteria. This phenomenon is attributed to the thicker cell wall of Gram-positive bacteria.

Notably, GOβL reached the half-life of degradation at around 12 h. Its characteristic peak was not observed at around 24 h because of the easy hydrolysis reaction of β-lactam with ring opening (Figure 5). This attribute strongly suggests that the synthesized GOβL can serve as an environmental disinfectant. Molecular simulations further revealed that the inhibition site of GOβL lies in the active serine (Ser307). As such, GOβL can block the channel before the active serine binding site and interrupt the cross-linking process, leaving the bacteria with an incomplete cell wall, thus achieving an inhibition effect (Figure 6). This study provides a fast and easy method for the synthesis of GOβL, which can be adopted as a simple preparation method of residue-free disinfectant. Nevertheless, electrochemical stripping introduced uncertainty in the degree of oxidation, resulting in an inconsistent ratio of ketene functional groups on the GO surface for each synthesis. These inconsistencies can prevent bacterial induction of β-lactamase production and should thus be explored in subsequent studies. Moreover, the analysis of GOβL inhibition sites is not very detailed, as we are currently unable to prove that the simulated

inhibition sites are correct through relevant experiments and therefore should be further explored in subsequent studies.

In recent years, graphene-based compounds have rapidly emerged as a promising category of antibacterial materials due to their diverse bactericidal mechanisms and relatively low cytotoxicity to mammalian cells.[36] In this study, we have synthesized GOβL with an antibacterial effect using GO nanomaterials. The combination of GO with other substances to produce antimicrobial nanocomposites is reportedly being investigated extensively,[36,37] and the nanomaterials obtained by combining Ag and Zn with GO have shown excellent antimicrobial activity,[38,39] with Ag/GO showing activity comparable to that of the penicillin-like β-lactam antibiotic ampicillin. With its unique mechanical and physicochemical properties, GO makes it particularly attractive for basic research and possible applications in many fields.[40] The GO composite can be used to treat wastewater with toxic inorganic and organic pollutants due to its large specific surface area, geometry, and chemical properties,[41] in addition to its bacterial inhibition, as described above. Simultaneously, the problem of secondary contamination by adsorbed toxic substances has to be taken into account, and they may pose serious health and environmental risks. Therefore, desorption and regeneration are important aspects of the commercialization of graphene-based nanomaterials.
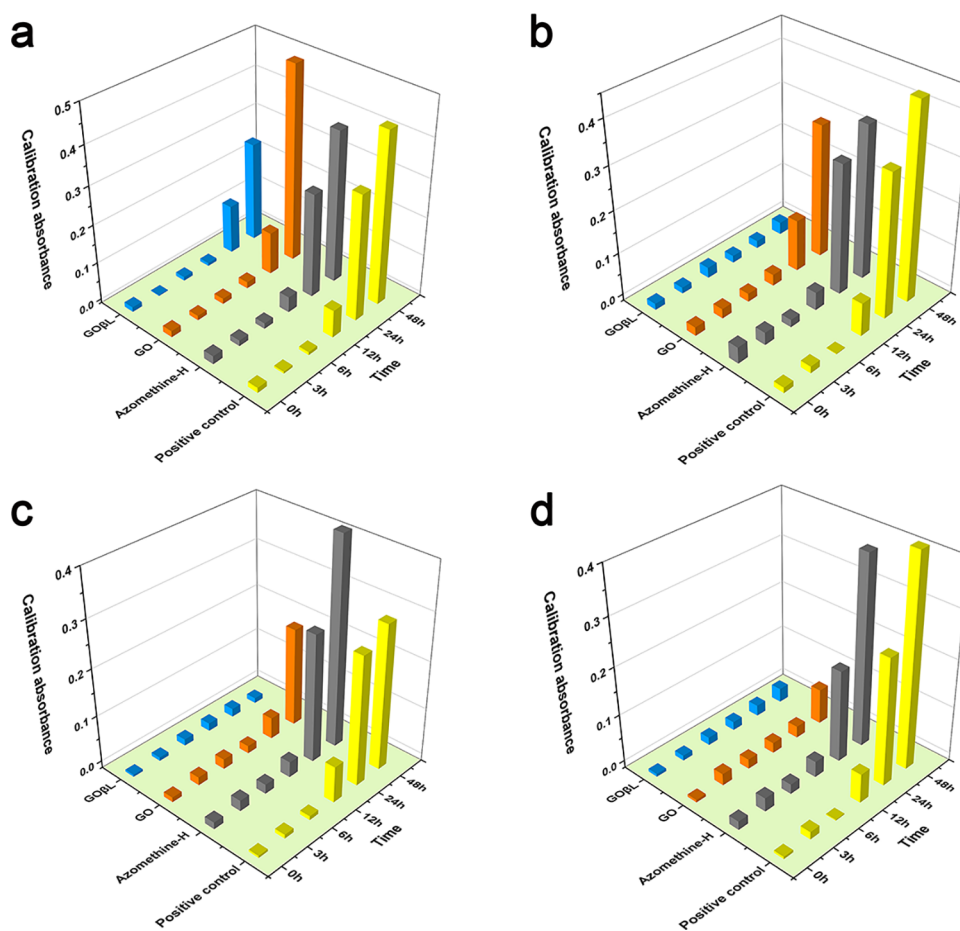
Figure 4. Relationship between the incubation time of environmental isolates and the bacterial inhibition effect of GOβL. Bacterial inhibition of *S. aureus* (a), *E. coli* (b), *S. enterica* (c), and *S. dysenteriae* (d) by GOβL (63.5 μg mL^{-1}) at different incubation times.
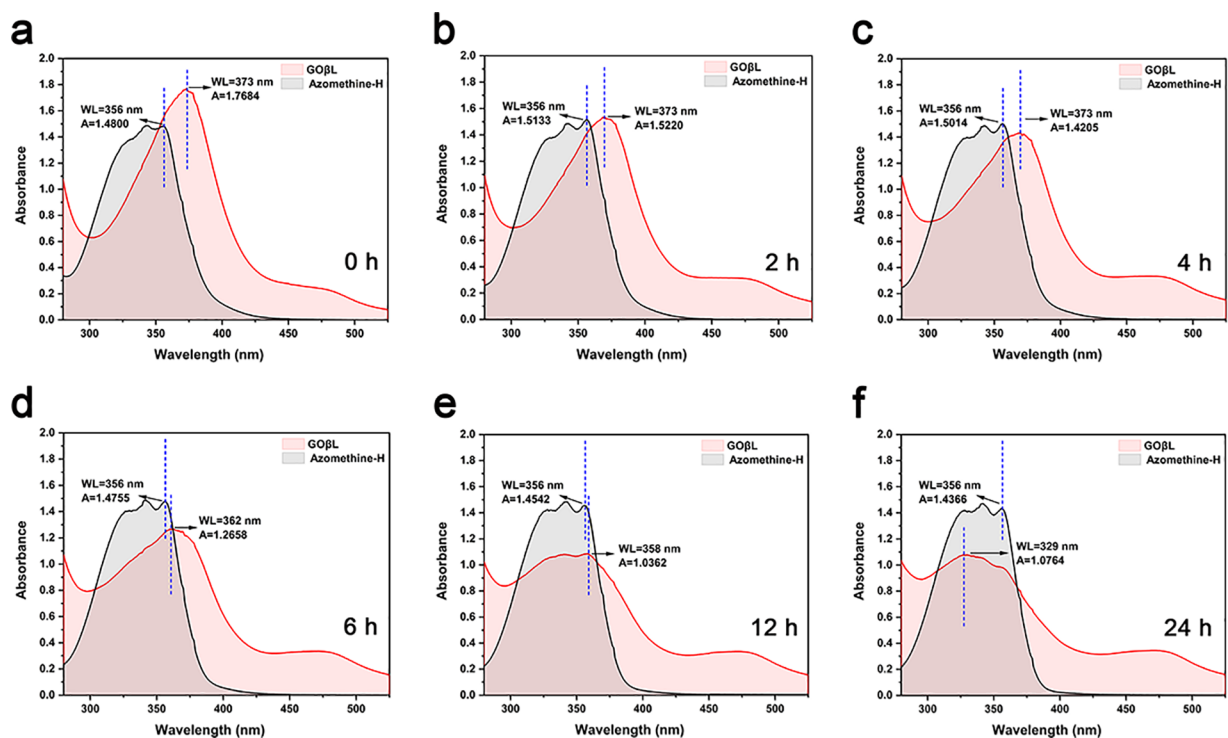
Figure 5. Time-varying degradation effect of GOβL. UV−vis absorption spectra of GOβL and azomethane-H deposited at 0 (a), 1 (b), 2 (c), 4 (d), 6 (e), and 12h (f).
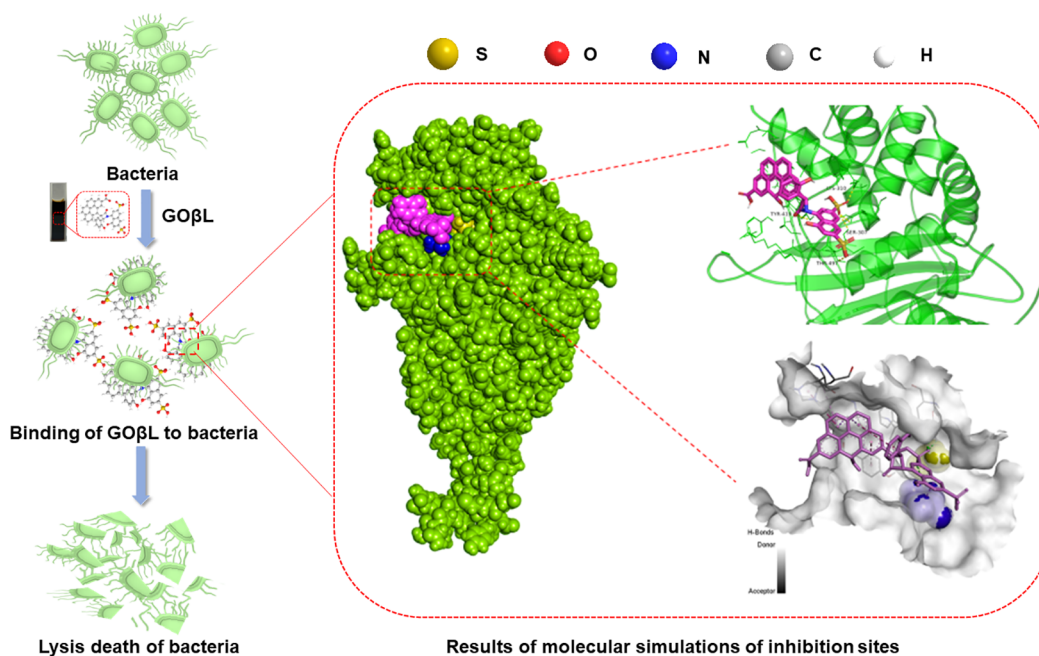
Figure 6. Schematic diagram of the inhibitory site of the simulated GOβL. Covalent binding of GOβL to the active serine (Ser307) of PBP3 in the bacterial cell wall.

5. CONCLUSION

In this study, we synthesized a GO rich in ketene functional groups and prepared GOβL via a [2 + 2] cycloaddition reaction with azomethine-H in the aqueous phase. GOβL can block the channel before the active serine binding site, interrupting the cross-linking process and rendering the bacterial cell wall incomplete, thus achieving inhibition. The synthesized GOβL exhibited a broad-spectrum bacterial inhibitory effect against common environmental pathogens within 24 h. Notably, the synthesized GOβL also degraded rapidly within 24 h. However, the large layer structure of GO allows the inhibition effect of GOβL to remain in place after 48 h. This study provides a rapid and simple method for the synthesis of GOβL, which can be adopted as a simple preparation method of residue-free environmental disinfectant.

■ ASSOCIATED CONTENT

ⓈⒾ Supporting Information

The Supporting Information is available free of charge at https://pubs.acs.org/doi/10.1021/acsomega.2c02328.

> High-resolution XPS of the C 1s spectra of pencil cores and GO powder (Figure S1); Raman spectrum of GO (Figure S2); UV absorption spectra and FT-IR absorption spectra of electrolytic solutions (Figure S3); reaction mechanism of monocyclic β-lactam (Figure S4); structure and IR spectra of esters obtained through B3LYP/6-31G(d) (Figure S5) (PDF)

■ AUTHOR INFORMATION

Corresponding Authors

Zhongzhu Yang − *State Key Laboratory of Southwestern Chinese Medicine Resources, College of Medical Technology, Chengdu University of Traditional Chinese Medicine, Chengdu, Sichuan 611137, China*; Email: yzz@cdutcm.edu.cn

Yang He − *State Key Laboratory of Southwestern Chinese Medicine Resources, College of Medical Technology, Chengdu University of Traditional Chinese Medicine, Chengdu, Sichuan 611137, China*; ⓘ orcid.org/0000-0003-0163-4307; Email: heyang@cdutcm.edu.cn

Authors

Chenyan Hu − *State Key Laboratory of Southwestern Chinese Medicine Resources, College of Medical Technology, Chengdu University of Traditional Chinese Medicine, Chengdu, Sichuan 611137, China; Department of Laboratory Medicine, People's Hospital of Xinjin District, Chengdu, Sichuan 611430, China*

Pengfei Heng − *State Key Laboratory of Southwestern Chinese Medicine Resources, College of Medical Technology, Chengdu University of Traditional Chinese Medicine, Chengdu, Sichuan 611137, China*

Yuanyuan Zeng − *State Key Laboratory of Southwestern Chinese Medicine Resources, College of Medical Technology, Chengdu University of Traditional Chinese Medicine, Chengdu, Sichuan 611137, China*

Qing Zhang − *Key Laboratory of Food Biotechnology, School of Food and Biotechnology, Xihua University, Chengdu, Sichuan 610039, China*

Meilian Zhao − *State Key Laboratory of Southwestern Chinese Medicine Resources, College of Medical Technology, Chengdu University of Traditional Chinese Medicine, Chengdu, Sichuan 611137, China*

Complete contact information is available at:
https://pubs.acs.org/10.1021/acsomega.2c02328

Author Contributions

Chenyan Hu: conceptualization, funding acquisition, investigation, supervision, writing original draft, writing−review and editing. Pengfei Heng: investigation, visualization, writing original draft, writing−review and editing. Yuanyuan Zeng: investigation, resources. Qing Zhang: data curation. Meilian

Zhao: visualization. Zhongzhu Yang: conceptualization, investigation, project administration, supervision, writing original draft, writing—review and editing. Yang He: conceptualization, investigation, project administration, writing—review and editing, supervision.

Author Contributions

⊥C.H. and P.H. contributed equally to this work.

Notes

The authors declare no competing financial interest.

■ REFERENCES

(1) Ferraresso, J.; Lawton, B.; Bayliss, S.; Sheppard, S.; Cardazzo, B.; Gaze, W.; Buckling, A.; Vos, M. Determining the Prevalence, Identity and Possible Origin of Bacterial Pathogens in Soil. *Environ. Microbiol.* **2020**, *22* (12), 5327−5340.

(2) Schirone, M.; Visciano, P.; Tofalo, R.; Suzzi, G. Editorial: Foodborne Pathogens: Hygiene and Safety. *Front. Microbiol.* **2019**, *10* (AUG), 1−4.

(3) McEwen, S. A.; Collignon, P. J. Antimicrobial Resistance: A One Health Colloquium. *Microbiol. Spectr.* **2018**, *6* (2), 1−26.

(4) Rozman, U.; Pusnik, M.; Kmetec, S.; Duh, D.; Sostar Turk, S. Reduced Susceptibility and Increased Resistance of Bacteria against Disinfectants: A Systematic Review. *Microorganisms* **2021**, *9* (12), 2550.

(5) Chapman, J. S. Disinfectant Resistance Mechanisms, Cross-Resistance, and Co-Resistance. *Int. Biodeterior. Biodegrad.* **2003**, *51* (4), 271−276.

(6) Vassallo, J.; Besinis, A.; Boden, R.; Handy, R. D. The Minimum Inhibitory Concentration (MIC) Assay with Escherichia Coli: An Early Tier in the Environmental Hazard Assessment of Nanomaterials? *Ecotoxicol. Environ. Saf.* **2018**, *162* (April), 633−646.

(7) Bush, K.; Bradford, P. A. β-Lactams and β-Lactamase Inhibitors: An Overview. *Cold Spring Harb. Perspect. Med.* **2016**, *6* (8), a025247.

(8) Davies, R.; Wales, A. Antimicrobial Resistance on Farms: A Review Including Biosecurity and the Potential Role of Disinfectants in Resistance Selection. *Compr. Rev. Food Sci. Food Saf.* **2019**, *18* (3), 753−774.

(9) Marti, S.; Puig, C.; Merlos, A.; Viñas, M.; de Jonge, M. I.; Liñares, J.; Ardanuy, C.; Langereis, J. D. Bacterial Lysis through Interference with Peptidoglycan Synthesis Increases Biofilm Formation by Nontypeable Haemophilus Influenzae. *mSphere* **2017**, *2* (1), No. e00329-16.

(10) Hosseyni, S.; Jarrahpour, A. Recent Advances in β-Lactam Synthesis. *Org. Biomol. Chem.* **2018**, *16* (38), 6840−6852.

(11) Aliyev, E.; Filiz, V.; Khan, M. M.; Lee, Y. J.; Abetz, C.; Abetz, V. Structural Characterization of Graphene Oxide: Surface Functional Groups and Fractionated Oxidative Debris. *Nanomaterials* **2019**, *9* (8), 1180.

(12) Yu, W.; Sisi, L.; Haiyan, Y.; Jie, L. Progress in the Functional Modification of Graphene/Graphene Oxide: A Review. *RSC Adv.* **2020**, *10* (26), 15328−15345.

(13) Qian, L.; Wang, H.; Yang, J.; Chen, X.; Chang, X.; Nan, Y.; He, Z.; Hu, P.; Wu, W.; Liu, T. Amino Acid Cross-Linked Graphene Oxide Membranes for Metal Ions Permeation, Insertion and Antibacterial Properties. *Membranes (Basel).* **2020**, *10* (10), 1−15.

(14) Zhang, W. H.; Yin, M. J.; Zhao, Q.; Jin, C. G.; Wang, N.; Ji, S.; Ritt, C. L.; Elimelech, M.; An, Q. F. Graphene Oxide Membranes with

(15) Sengupta, I.; Bhattacharya, P.; Talukdar, M.; Neogi, S.; Pal, S. K.; Chakraborty, S. Bactericidal Effect of Graphene Oxide and Reduced Graphene Oxide: Influence of Shape of Bacteria. *Colloids Interface Sci. Commun.* **2019**, *28*, 60−68.

(16) Jiang, N.; Wang, Y.; Chan, K. C.; Chan, C.; Sun, H.; Li, G. Additive Manufactured Graphene Coating with Synergistic Photothermal and Superhydrophobic Effects for Bactericidal Applications. *Glob. Challenges* **2020**, *4* (1), 1900054.

(17) Lima, L. M.; Silva, B. N. M. da; Barbosa, G.; Barreiro, E. J. β-Lactam Antibiotics: An Overview from a Medicinal Chemistry Perspective. *Eur. J. Med. Chem.* **2020**, *208*, 112829.

(18) García-Dalí, S.; Paredes, J. I.; Munuera, J. M.; Villar-Rodil, S.; Martínez-Alonso, A.; Tascón, J. M. D. An Aqueous Cathodic Delamination Route towards High Quality Graphene Flakes for Oil Sorption and Electrochemical Charge Storage Applications. *Chem. Eng. J.* **2019**, *372*, 1226−1239.

(19) Jarrahpour, A.; Doroodmand, M. M.; Ebrahimi, E. The First Report of [2 + 2] Ketene-Imine Cycloaddition Reactions (Staudinger) on Carbon Nanotubes. *Tetrahedron Lett.* **2012**, *53* (23), 2797−2801.

(20) Costa, M. C. F.; Marangoni, V. S.; Ng, P. R.; Nguyen, H. T. L.; Carvalho, A.; Castro Neto, A. H. Accelerated Synthesis of Graphene Oxide from Graphene. *Nanomaterials* **2021**, *11* (2), 551.

(21) Decuyper, L.; Jukič, M.; Sosič, I.; Žula, A.; D'hooghe, M.; Gobec, S. Antibacterial and β-Lactamase Inhibitory Activity of Monocyclic β-Lactams. *Med. Res. Rev.* **2018**, *38* (2), 426−503.

(22) Wang, J.; Shan, Z.; Tan, X.; Li, X.; Jiang, Z.; Qin, J. Preparation of Graphene Oxide (GO)/Lanthanum Coordination Polymers for Enhancement of Bactericidal Activity. *J. Mater. Chem. B* **2021**, *9* (2), 366−372.

(23) Parthipan, P.; Cheng, L.; Rajasekar, A.; Govarthanan, M.; Subramania, A. Biologically Reduced Graphene Oxide as a Green and Easily Available Photocatalyst for Degradation of Organic Dyes. *Environ. Res.* **2021**, *196*, 110983.

(24) Shams, M.; Guiney, L. M.; Huang, L.; Ramesh, M.; Yang, X.; Hersam, M. C.; Chowdhury, I. Influence of Functional Groups on the Degradation of Graphene Oxide Nanomaterials. *Environ. Sci. Nano* **2019**, *6* (7), 2203−2214.

(25) Frisch, M. J.; Trucks, G. W.; Schlegel, H. B.; Scuseria, G. E.; Robb, M. A.; Cheeseman, J. R.; Scalmani, G.; Barone, V.; Mennucci, B.; Petersson, G. A.; Nakatsuji, H.; Caricato, M.; Li, X.; Hratchian, H. P.; Izmaylov, A. F.; Bloino, J.; Zheng, G.; Sonnenberg, J. L.; Hada, M.; Ehara, M.; Toyota, K.; Fukuda, R.; Hasegawa, J.; Ishida, M.; Nakajima, T.; Honda, Y.; Kitao, O.; Nakai, H.; Vreven, T.; Montgomery, J. A. J.; Peralta, J. E.; Ogliaro, F.; Bearpark, M.; Heyd, J. J.; Brothers, E.; Kudin, K. N.; Staroverov, V. N.; Kobayashi, R.; Normand, J.; Raghavachari, K.; Rendell, A.; Burant, J. C.; Iyengar, S. S.; Tomasi, J.; Cossi, M.; Rega, N.; Millam, J. M.; Klene, M.; Knox, J. E.; Cross, J. B.; Bakken, V.; Adamo, C.; Jaramillo, J.; Gomperts, R.; Stratmann, R. E.; Yazyev, O.; Austin, A. J.; Cammi, R.; Pomelli, C.; Ochterski, J. W.; Martin, R. L.; Morokuma, K.; Zakrzewski, V. G.; Voth, G. A.; Salvador, P.; Dannenberg, J. J.; Dapprich, S.; Daniels, A. D.; Farkas, Ö.; Foresman, J. B.; Ortiz, J. V; Cioslowski, J.; Fox, D. J. *Gaussian 09*; Gaussian Inc.: Wallingford, CT, 2009.

(26) Bush, K.; Bradford, P. A. Bush and Bradford - 2016 - β-Lactams and β-Lactamase Inhibitors An Overview.Pdf. *Cold Spring Harb. Perspect. Meddicine* **2016**, *6*, a025247.

(27) Brem, J.; Cain, R.; Cahill, S.; McDonough, M. A.; Clifton, I. J.; Jiménez-Castellanos, J. C.; Avison, M. B.; Spencer, J.; Fishwick, C. W. G.; Schofield, C. J. Structural Basis of Metallo-β-Lactamase, Serine-β-Lactamase and Penicillin-Binding Protein Inhibition by Cyclic Boronates. *Nat. Commun.* **2016**, *7*, 1−8.

(28) Farley, A. J. M.; Ermolovich, Y.; Calvopiña, K.; Rabe, P.; Panduwawala, T.; Brem, J.; Björkling, F.; Schofield, C. J. Structural Basis of Metallo-β-Lactamase Inhibition by N-Sulfamoylpyrrole-2-Carboxylates. *ACS Infect. Dis.* **2021**, *7* (6), 1809−1817.

(29) Tooke, C. L.; Hinchliffe, P.; Lang, P. A.; Mulholland, A. J.; Brem, J.; Schofield, C. J.; Spencer, J. Molecular Basis of Class A β-Lactamase Inhibition by Relebactam. *Antimicrob. Agents Chemother.* **2019**, *63* (10), No. e00564-19.

(30) Jubeh, B.; Breijyeh, Z.; Karaman, R. Resistance of Gram-Positive Bacteria to Current Antibacterial Agents and Overcoming Approaches. *Molecules* **2020**, *25* (12), 2888.

(31) Chen, Z.; Guo, J.; Jiang, Y.; Shao, Y. High Concentration and High Dose of Disinfectants and Antibiotics Used during the COVID-19 Pandemic Threaten Human Health. *Environ. Sci. Eur.* **2021**, *33* (1), 11.

(32) Ghafoor, D.; Khan, Z.; Khan, A.; Ualiyeva, D.; Zaman, N. Excessive Use of Disinfectants against COVID-19 Posing a Potential Threat to Living Beings. *Curr. Res. Toxicol.* **2021**, *2*, 159−168.

(33) Dhama, K.; Patel, S. K.; Kumar, R.; Masand, R.; Rana, J.; Yatoo, M. I.; Tiwari, R.; Sharun, K.; Mohapatra, R. K.; Natesan, S.; Dhawan, M.; Ahmad, T.; Emran, T. B.; Malik, Y. S.; Harapan, H. The Role of Disinfectants and Sanitizers during COVID-19 Pandemic: Advantages and Deleterious Effects on Humans and the Environment. *Environ. Sci. Pollut. Res.* **2021**, *28* (26), 34211−34228.

(34) Rai, N. K.; Ashok, A.; Akondi, B. R. Consequences of Chemical Impact of Disinfectants: Safe Preventive Measures against COVID-19. *Crit. Rev. Toxicol.* **2020**, *50* (6), 513−520.

(35) Sultan, I.; Rahman, S.; Jan, A. T.; Siddiqui, M. T.; Mondal, A. H.; Haq, Q. M. R. Antibiotics, Resistome and Resistance Mechanisms: A Bacterial Perspective. *Front. Microbiol.* **2018**, *9*, 2066.

(36) Rojas-Andrade, M. D.; Chata, G.; Rouholiman, D.; Liu, J.; Saltikov, C.; Chen, S. Antibacterial Mechanisms of Graphene-Based Composite Nanomaterials. *Nanoscale* **2017**, *9* (3), 994−1006.

(37) Nichols, F.; Chen, S. Graphene Oxide Quantum Dot-Based Functional Nanomaterials for Effective Antimicrobial Applications. *Chem. Rec.* **2020**, *20* (12), 1505−1515.

(38) Xu, W. P.; Zhang, L. C.; Li, J. P.; Lu, Y.; Li, H. H.; Ma, Y. N.; Wang, W. Di; Yu, S. H. Facile Synthesis of Silver@graphene Oxide Nanocomposites and Their Enhanced Antibacterial Properties. *J. Mater. Chem.* **2011**, *21* (12), 4593−4597.

(39) Tang, J.; Chen, Q.; Xu, L.; Zhang, S.; Feng, L.; Cheng, L.; Xu, H.; Liu, Z.; Peng, R. Graphene Oxide-Silver Nanocomposite As a Highly Effective. *ACS Appl. Mater. Interfaces* **2013**, *5*, 3867−3874.

(40) Wang, S.; Sun, H.; Ang, H. M.; Tadé, M. O. Adsorptive Remediation of Environmental Pollutants Using Novel Graphene-Based Nanomaterials. *Chem. Eng. J.* **2013**, *226* (June), 336−347.

(41) Ali, I.; Basheer, A. A.; Mbianda, X. Y.; Burakov, A.; Galunin, E.; Burakova, I.; Mkrtchyan, E.; Tkachev, A.; Grachev, V. Graphene Based Adsorbents for Remediation of Noxious Pollutants from Wastewater. *Environ. Int.* **2019**, *127* (March), 160−180.